Applied Physics Letters

# Tunability and switching of Fano and Lorentz resonances in *PTX*-symmetric electronic systems

Cite as: Appl. Phys. Lett. **117**, 031101 (2020); https://doi.org/10.1063/5.0014919
Submitted: 22 May 2020 . Accepted: 06 July 2020 . Published Online: 20 July 2020

Zhilu Ye, Mohamed Farhat, and Pai-Yen Chen

View Online Export Citation CrossMark

ARTICLES YOU MAY BE INTERESTED IN

Perspective of self-assembled InGaAs quantum-dots for multi-source quantum implementations
Applied Physics Letters **117**, 030501 (2020); https://doi.org/10.1063/5.0010782

Design principles of dual-functional molecular switches in solid-state tunnel junctions
Applied Physics Letters **117**, 030502 (2020); https://doi.org/10.1063/5.0016280

Single-shot wavelength-multiplexed digital holography for 3D fluorescent microscopy and other imaging modalities
Applied Physics Letters **117**, 031102 (2020); https://doi.org/10.1063/5.0011075

Lock-in Amplifiers up to 600 MHz
Watch



© 2020 Author(s).

Applied Physics Letters ARTICLE scitation.org/journal/apl

# Tunability and switching of Fano and Lorentz resonances in *PTX*-symmetric electronic systems

Cite as: Appl. Phys. Lett. **117**, 031101 (2020); doi: 10.1063/5.0014919
Submitted: 22 May 2020 · Accepted: 6 July 2020 ·
Published Online: 20 July 2020

View Online Export Citation CrossMark

Zhilu Ye,[1] Mohamed Farhat,[2] and Pai-Yen Chen[1,a)]

## AFFILIATIONS

[1]Department of Electrical and Computer Engineering, University of Illinois at Chicago, Chicago, Illinois 60607, USA
[2]Computer, Electrical, and Mathematical Science and Engineering Division, King Abdullah University of Science and Technology, Thuwal 23955, Saudi Arabia

[a)]Author to whom correspondence should be addressed: pychen@uic.edu

## ABSTRACT

Resonance is a ubiquitous phenomenon observed in a wide range of physical systems. Recently, with the Fano resonance exerting remarkable potential for optical, acoustic, atomic, and electronic applications, it is vital to control and even dynamically reconfigure the resonance line shape and bandwidth, in addition to its frequency. In this work, we introduce a parity-time-reciprocal scaling (*PTX*)-symmetric structure, which can offer a promising avenue for tailoring the resonance frequency and line shape of electronic circuits. We have theoretically studied the resonance behavior of such a *PTX*-symmetric electronic system, particularly for dependencies of resonant peaks and line-shapes on the non-Hermiticity, coupling coefficient, and the scaling coefficient introduced by the reciprocal scaling ($X$) transformation. Our results demonstrate that, at resonance frequencies, a transition between Fano and Lorentzian line-shapes is possible with a specific reciprocal scaling rule applied to lumped-element circuits.

*Published under license by AIP Publishing.* https://doi.org/10.1063/5.0014919

Resonance is a fundamental phenomenon in several physical fields, such as optics, electronics, electromagnetics, acoustics, elastodynamics, and quantum mechanics, to name a few.[1] The Lorentzian resonance with a symmetric line shape was regarded as the fundamental line shape of a typical resonance,[2] which is generally realized in a single oscillator with an external applied harmonic force. In 1961, Ugo Fano discovered a new type of resonance which exhibits an asymmetric line shape, so-called Fano resonance.[3] Such a spectral feature was observed in a system consisting of two weakly coupled oscillators (only one oscillator is driven by an external force) and can be described by the well-known Fano formula.[4] In this class of resonators, the Fano parameter $q$ measuring the degree of asymmetry is usually used to describe the transition between Fano and Lorentzian line-shapes. It has been proven that when the coupling parameter $q$ becomes very strong ($q \to \pm\infty$) or $q$ tends to zero, the Fano profile reduces to a symmetric Lorentzian line shape.[5] Recently, it was suggested that the Fano resonance and its enabled electromagnetically induced transparency (EIT) can be generated at optical frequencies using plasmonic structures,[6] optical nanocircuits,[7] and microwave lumped-element circuitry,[8] or even in acoustics.[9] The Fano resonance is generated when two resonant modes (one discrete and one broadband) interfere with each other, and the out-of-phase coupling between the modes (destructive interference) may lead to EIT. Thus, the Fano resonance and EIT have become topics of intense interest due to their promising optical and microwave applications, such as slow light devices,[10] narrow-band filtering, bio- and chemical sensing,[10–12] optical switching,[13,14] and enhancement of nonlinear wave mixing.[15–17] In this context, electronic circuits have been exploited to elucidate the mechanisms of Fano and Lorentzian resonances,[8,18] as they are considered as an effective-mapping image of classical mechanics and also bring about new applications, such as the effective linewidth tuning for microwave filters and oscillators, as well as sensors with improved sensitivity and resolvability.[8,19–21]

In this work, we introduce the parity-time-reciprocal scaling (*PTX*)-symmetric electronic systems, aiming to realize resonances transitioning from Lorentzian to Fano line-shapes at the frequency of interest (that is also tunable). Parity-time (*PT*)-symmetry was first discovered by Bender and Boettcher in quantum mechanics.[22] Since then, *PT*-symmetry has aroused intense interest in fields of optics and photonics,[23–28] acoustics,[29,30] electromagnetics,[31–34] and electronics.[35–43] Except for being mathematically and physically intriguing, *PT*-symmetric systems enable many new applications, such as unidirectional reflectionless wave propagation,[23,24,44,45] invisibility cloaks,[46,47] negative refraction,[48] ultrahigh-sensitivity sensors enabled by


Published under license by AIP Publishing

eigenvalue bifurcation,[49–52] and coherent perfect absorber-lasers.[53,54] Counterintuitively, even though a *PT*-symmetric system is described by a non-Hermitian Hamiltonian, it can exhibit entirely real eigenspectra, provided that the system is invariant under combined parity and time-reversal transformations. Recently, we have proposed the generalized *PT*-symmetric (or *PTX*-symmetric) electronic system and its telemetric sensing applications.[42,43] The *PTX*-symmetric electronic system shown schematically in Fig. 1 consists of an active $-RLC$ oscillator (where $-R$ can be realized with a negative-resistance converter or NRC[43]) and a passive *RLC* oscillator, which are inductively coupled to achieve a spatially-varying gain and loss profile. Specifically, such a system is invariant under the combined parity transformation $P$ $(q_1 \to q_2)$, time-reversal transformation $T$ $(t \to -t)$, and the reciprocal scaling transformation $X\,(q_1 \to (m/n)^{1/2} q_1,\ q_2 \to (m/n)^{-1/2} q_2)$, where $q_1\,(q_2)$ corresponds to the charge stored in the capacitor in the $-RLC\,(RLC)$ tank and the scaling coefficients $m$ and $n$ are arbitrary positive real numbers. Different from *PT*-symmetric systems, the *PTX*-symmetric one may possess unequal gain and loss coefficients, i.e., $-mR$ and $nR$, as shown in Fig. 1; this system degenerates into its *PT* counterpart if $m = n$. More importantly, the $X$ transformation offers the possibility for engineering the line shape and bandwidth ($Q$-factor) of resonances, which can transit between the Fano and the Lorentzian spectral line-shapes. In this Letter, we theoretically study the characteristics of resonance in the *PTX*-symmetric electronic circuit shown in Fig. 1, which consists of lumped elements operating in radio-frequency (RF) and microwave regions. Nevertheless, the concept may be extended to the optical region by means of the optical nanocircuit theorem.[48] As detailed next, with this scaling coefficient, a Fano-to-Lorentzian transition accompanied by a tunable linewidth can be obtained, with the operation frequencies controlled by the gain-loss parameter (non-Hermiticity) and the coupling coefficient in the *PTX*-symmetric system. The proposed *PTX*-symmetric system may be likewise realized in terahertz

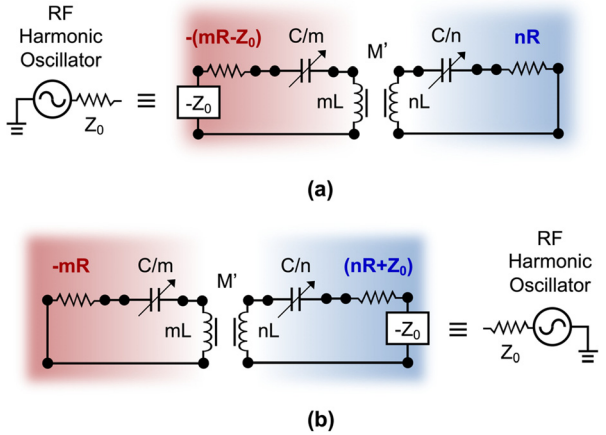


**FIG. 1.** Illustration of the proposed *PTX*-symmetric electronic system excited by a harmonic oscillator connected to (a) the gain side and (b) the loss side. Here, $m$ and $n$ are the scaling coefficients. If $m = n = 1$, the *PTX* system degenerates into the *PT*-symmetric one. In the steady state, an AC signal generator producing continuous-wave sinusoidal signals is represented by $-Z_0$, where $Z_0$ is the source (generator) impedance.

and optical frequencies by exploiting the photoexcited thin-layer with gain [such as some two-dimensional (2D) materials,[32] polymers, or III–V semiconductors[54]] and the resistive filament, within the realm of optical nanocircuit.

The *PTX*-symmetric electronic system based on the lumped-element circuit (Fig. 1) is similar to its *PT*-symmetric counterpart $(m = n = 1)$, but all elements are scaled according to the following rule: $-R \to -mR$, $L \to mL$, and $C \to m^{-1}C$ on the gain side, while $R \to nR$, $L \to nL$, and $C \to n^{-1}C$ on the loss side. Applying Kirchhoff's laws to this circuit, the system can be described by an effective non-Hermitian Hamiltonian $H_{\rm eff}\mathbf{\Psi} = i\partial_\tau \mathbf{\Psi}$, where $\mathbf{\Psi} = (q_1, q_2, \dot{q}_1, \dot{q}_2)^T$, $\tau \equiv \omega_0 t$, and the angular oscillation frequency of a neutral *LC* tank ($\omega_0 = 1/\sqrt{LC}$[43]) (see the supplementary material). When a time-harmonic sinusoidal excitation is connected to the $-RLC$ or *RLC* oscillator, the forced oscillations arise in the system. In the normal mode analysis, while a positive resistance implies energy dissipation, an energy source (AC signal generator) with a generator impedance $Z_0$ is seen as a negative resistance, i.e., $-Z_0$. Therefore, if the signal generator is connected to the series $-RLC$ tank, an NRC with an equivalent resistance of $-(mR - Z_0)$ and a resistor with a resistance of $R$ must be adopted, such that the *PTX*-symmetry condition is preserved. On the other hand, when an AC signal generator is connected to the *RLC* tank, a resistor with a resistance of $nR + Z_0$ and an NRC with a resistance of $-mR$ must be used in the *PTX*-symmetric circuit. The electronic circuits in Fig. 1 have four eigenfrequencies (in units of $\omega_0$) that can be obtained from the eigenvalue problem: $(H_{\rm eff} - \omega_i \mathbf{I})\mathbf{\Psi} = 0$, and they can be written as (see the supplementary material)

$$\omega_{1,2,3,4} = \pm\omega_0 \sqrt{\frac{2\gamma^2 - 1 \pm \sqrt{1 - 4\gamma^2 + 4\gamma^4\kappa^2}}{2\gamma^2(1-\kappa^2)}}, \tag{1}$$

where the gain-loss parameter (or non-Hermiticity) $\gamma = R^{-1}\sqrt{L/C}$, the coupling coefficient $\kappa = M/L$, and $M$ is the mutual inductance between the two oscillators. There is a redundancy in Eq. (1) because positive and negative eigenfrequencies of equal magnitude are essentially identical. These eigenfrequencies bifurcate and branch out into the complex plane at the two exceptional points, and the one governing the exact symmetry and broken phases is given by

$$\gamma_{\rm EP} = \frac{1}{\kappa}\sqrt{\frac{1 + \sqrt{1-\kappa^2}}{2}}. \tag{2}$$

From Eq. (1), we find that the *PTX*-symmetric system and *PT*-symmetric one display the same eigenspectra, even though the gain and loss coefficients are not necessarily the same (i.e., $|-mR| \neq nR$). More interestingly, the eigenfrequencies are independent of the scaling factors $m$ and $n$. Similar to *PT*-symmetric systems, phase transitions (which are determined by $\gamma$ and $\kappa$) are also found in the *PTX*-symmetric system, as shown in Fig. 2. In fact, the Hamiltonian and the eigenmodes of the *PTX*-symmetric electronic system in Fig. 1 may be related to those of the *PT*-symmetric system $(H', \mathbf{\Psi}')$ through the similarity transformation: $H = S^{-1}H'S$ and $\mathbf{\Psi} = S^{-1}\mathbf{\Psi}'$, where $S$ is an invertible 4-by-4 matrix.[43] As a result, *PTX* and *PT* systems may share the same eigenfrequencies, but may possess dissimilar eigenmodes. Moreover, $H$ commutes with the transformed operators $\check{P} = S^{-1}PS$ and $\check{T} = S^{-1}TS = T$, i.e., $[\check{P}\check{T}, H] = 0$ where $\check{P}$ performs the


Published under license by AIP Publishing

combined operations of parity and reciprocal scaling: $(m/n)^{1/2} q_1 \leftrightarrow (m/n)^{-1/2} q_2$ ($\breve{P}\breve{T} = PTX$). We should note that $PTX$-symmetry can be considered as the generalized $PT$-symmetry, as it degenerates into the $PT$ form when $m = n = 1$. In the $PTX$-symmetric system, $\gamma$ and $\kappa$ are responsible for the eigenfrequencies and eigenmodes, whereas scaling coefficients $m$ and $n$ can tune the resonance line-shapes.

Under the single-port excitation, the information (e.g., sensor applications) may be encoded in the reflection coefficient $r$. When the $PTX$-symmetric circuit is driven by a sinusoidal source connected to the $-RLC$ tank, the reflectance $R_G$ observed from the gain side is given by

$$R_G = r_G \cdot r_G^* = \frac{\left(\prod_{i=1}^{4} \omega - \omega_i / \Gamma(\omega)\right)^2}{C_0^2 + \left(\prod_{i=1}^{4} \omega - \omega_i / \Gamma(\omega) + \alpha\right)^2}, \tag{3}$$

where $\alpha = \eta/m$, $\Gamma(\omega) = 2\omega^2/[\gamma^2(\kappa^2 - 1)]$ which describes the resonance width, $C_0 = \alpha\gamma(\omega - 1/\omega)$, $\eta = Z_0/R$, and $\omega_i$ is the $i$-th eigenfrequency in Eq. (1). The reflectance observed from the loss side can be similarly written as

$$R_L = r_L \cdot r_L^* = \frac{\left(\prod_{i=1}^{4} \omega - \omega_i / \Gamma(\omega)\right)^2}{D_0^2 + \left(\prod_{i=1}^{4} \omega - \omega_i / \Gamma(\omega) - \beta\right)^2}, \tag{4}$$

where $\beta = \eta/n$ and $D_0 = \beta\gamma(\omega - 1/\omega)$. Equations (3) and (4) reveal that in the exact $PT$-symmetric phase where $\gamma > \gamma_{EP}$ and $\omega_i$ is purely real, resonant reflection dips (i.e., $R_G, R_L = 0$) are obtained at the eigenfrequencies in the reflection spectra [Eq. (1)] shown in Fig. 2. The formulas stating the resonance behavior of this $PTX$-symmetric system can be equivalent to the modified Fano or Lorentzian resonance model. Here, $\alpha$ and $\beta$, respectively, related to the scaling coefficients $m$ and $n$, play critical roles in analogy to the Fano factor $q$ (which determines the spectral features of the resonance). From Eqs. (3) and (4), we also find that $R_G$ is independent of $n$, whereas $R_L$ is independent of $m$.

Figure 3(a) shows the reflectance spectra $R_G$ as a function of the normalized frequency $(\omega/\omega_0)$ under similar conditions ($\eta = 1$, $\kappa = 0.5$, $m = 2$, and $n$ is an arbitrary positive real number), but with different $\gamma$ (or $\Delta\gamma = \gamma - \gamma_{EP}$) in the exact $PT$-symmetric phase. From Fig. 3(a), it is evident that increasing $\Delta\gamma$ will cause a redshift (blueshift) for the resonance at a lower (higher) frequency, whose bifurcation loci are consistent with the results in Fig. 2. We note that the operation frequencies split rapidly nearby the exceptional point, and they coincide at the exceptional point ($\Delta\gamma = 0$). Figure 3(b) shows the reflectance spectra $R_G$ under similar conditions ($\eta = 1$, $\gamma = 5$, $m = 4$, and $n$ is an arbitrary positive real number), but with different $\kappa$ in the exact $PT$-symmetric phase. As can be observed in Fig. 3(b), the two resonance frequencies can be tuned by varying $\kappa$. The resonant peaks are, however, independent of $m$ and $n$. In practice, $\kappa$ and $\gamma$ may be tuned by simply adjusting the inductive coupling strength ($M$) and the values of the lumped elements ($R$, $L$, and $C$), respectively.

Next, we will discuss how the $X$ transformation in the generalized $PT$-symmetric circuit can be exploited to tailor the line-shapes of the two resonances. Figure 4(a) presents the contours of reflectance $R_G$ as a function of the normalized frequency and the scaling coefficient $m$; here, $\eta = 1$, $\kappa = 0.4$, $\gamma = 4$, and $n$ is an arbitrary positive real number. From Fig. 4(a), we find that the resonance line shape evolves from Lorentzian to Fano kinds by increasing the value of $m$. Particularly, we should emphasize that there exists a critical scaling coefficient that determines the type of resonance. For the first resonant mode observed at the lower frequency, if $|-mR| > Z_0$ (which yields an active circuit with $\alpha < 1$), $R_G$ displays a Fano-like resonance line shape and $R_G > 1$ is observed in some frequency ranges. On the other hand, if $|-mR| < Z_0$, (which yields a fully-passive circuit with $\alpha > 1$), this mode displays a Lorentzian resonance. For the second resonance mode observed at the higher frequency, if $-(mR - Z_0) < -(\kappa\sqrt{m})^2 R$ (or, equivalently, $\alpha < 1 - \kappa^2$) the active circuit displays a Fano-like line shape, while a Lorentzian line shape is obtained if $-(mR - Z_0) > -(\kappa\sqrt{m})^2 R$ or $\alpha > 1 - \kappa^2$. The critical scaling coefficient can also be obtained mathematically by observing the inequality $R_G > 1$ around the operation frequency. From Fig. 4(a), it is evident that in the $PTX$-symmetric system, the linewidths of both resonant modes decrease with increasing the value of $m$, and that above the critical value of $m$ [highlighted in Fig. 4(a)], a Lorentzian to Fano transition is observed. We also note that $R_G$ is not influenced by $n$, as can be

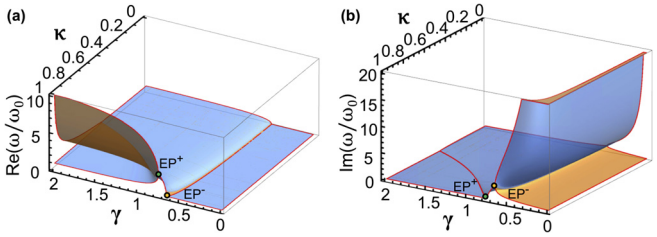


**FIG. 2.** Contours of (a) real and (b) imaginary parts of eigenfrequencies as functions of the non-Hermiticity parameter $\gamma$ and the coupling coefficient $\kappa$ for the $PTX$-symmetric circuit shown in Fig. 1. There exist two exceptional (branch) points, $\gamma_{EP^{\pm}} = \sqrt{(1 \pm \sqrt{1 - \kappa^2})/(2\kappa^2)}$ where the bifurcation occurs.

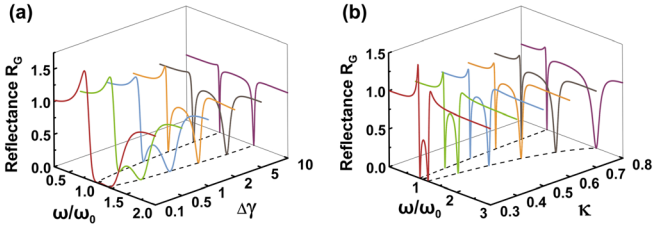


**FIG. 3.** (a) Resonance spectra of reflectance $R_G$ with different non-Hermiticity parameter $\Delta\gamma$, where $\Delta\gamma = \gamma - \gamma_{EP}$. If $\Delta\gamma$ is sufficiently small, the two resonance modes are coupled together. (b) Resonance spectra of reflectance $R_G$ with different coupling coefficient $\kappa$. Tunable operation frequency and resonance width are observed in both (a) and (b).


Published under license by AIP Publishing

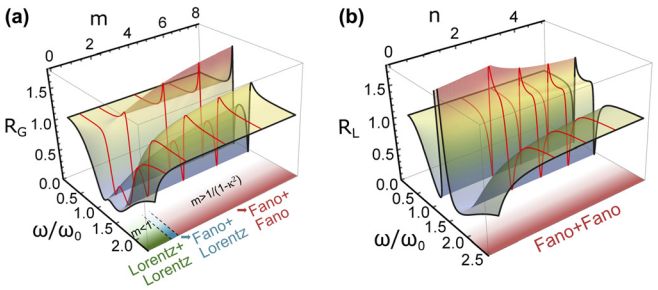


**FIG. 4.** (a) Resonance spectra of $R_G$ vs the scaling factor $m$ and normalized frequency $\omega/\omega_0$. By increasing $m$ (decreasing $\alpha$), a Lorentzian to Fano transition is observed and highlighted. (b) Resonance spectra of $R_L$ vs the scaling factor $n$ and normalized frequency $\omega/\omega_0$, from which Fano resonances are always obtained.

deduced from Eq. (3). Despite the tunability in linewidth, the resonance frequencies are always locked at $\omega_i$, regardless of the changes in $m$ and $n$. This is due to the fact that $PTX$ and $PT$ systems share the same eigenfrequencies that are tunable only with respect to $\gamma$ and $\kappa$.

Figure 4(b) depicts the resonance spectra of reflectance $R_L$ under different scaling factor $n$ when $\eta = 1$, $\kappa = 0.5$, $\gamma = 5$, showing that no matter how $n$ is varied, a Fano resonance line shape is always obtained. In this case, since an NRC with a resistance of $-mR$ must be used to maintain the $PTX$ symmetry, the electronic circuit is active and, therefore, the Lorentzian resonance is absent. In this case, the reflectance $R_L$ is insensitive to the changes in $m$. From Figs. 4(a) and 4(b), we find that the resonance linewidth is inversely proportional to the scaling coefficient $m$ or $n$, which describes the degree of asymmetry of the Fano-like resonances locked at $\omega_i$. Furthermore, for $R_G$, the newly introduced $X$ transformation enables switching the resonance between Fano and Lorentzian kinds at a fixed operating frequency. In practice, the tunable scaling coefficients $m$ and $n$ can be readily implemented by using variable lumped elements (e.g., trimmer potentiometers or varactor) that can be programmed via the external circuitry. Our findings open up unique possibilities for sharpening of resonance and effectively tuning the bandwidth ($Q$-factor) for various near-field sensing and communication applications.

To sum up, we have introduced the $PTX$-symmetric electronic system, in which the resonance frequencies are tunable with respect to the gain-loss parameter and the coupling coefficient, and resonance lineshapes may be altered by the scaling coefficient responsible for the $X$ transformation. In particular, the formulas that describe the spectral reflectance of this $PTX$-symmetric system can be cast into a Fano-like or a Lorentzian-like line shape by reconfiguring each lumped element ($\pm R$, $L$, and $C$). We have also derived the critical scaling coefficient that determines the transition from Fano to Lorentzian resonance at a fixed resonance frequency. The proposed $PTX$-symmetric circuit, capable of dynamically manipulating the central frequency, line shape, and linewidth of resonance, may open a new avenue for building advanced oscillator/resonator circuits, ultrahigh-resolution high-sensitivity sensors, and a more readily available platform for studying Fano resonances.

See the supplementary material for details on the Liouville formalism and effective Hamiltonian as well as the reflection from the PTX-symmetric circuit.

This material is based upon work supported by the National Science Foundation under Grant No. 1917678.

## DATA AVAILABILITY

The data that support the findings of this study are available from the corresponding author upon reasonable request.

## REFERENCES

[1]J. Walker, R. Resnick, and D. Halliday, *Fundamentals of Physics*, 10th ed. (Wiley, Hoboken, NJ, 2014).
[2]L. Petrakis, J. Chem. Educ. **44**, 432 (1967).
[3]U. Fano, Phys. Rev. **124**, 1866 (1961).
[4]A. E. Miroshnichenko, S. Flach, and Y. S. Kivshar, Rev. Mod. Phys. **82**, 2257 (2010).
[5]M. F. Limonov, M. V. Rybin, A. N. Poddubny, and Y. S. Kivshar, Nat. Photonics **11**, 543 (2017).
[6]B. Luk'yanchuk, N. I. Zheludev, S. A. Maier, N. J. Halas, P. Nordlander, H. Giessen, and C. T. Chong, Nat. Mater. **9**, 707 (2010).
[7]A. Li and W. Bogaerts, Opt. Express **25**, 31688 (2017).
[8]B. Lv, R. Li, J. Fu, Q. Wu, K. Zhang, W. Chen, Z. Wang, and R. Ma, Sci. Rep. **6**(1), 31884 (2016).
[9]M. Amin, A. Elayouch, M. Farhat, M. Addouche, A. Khelif, and H. Bağcı, J. Appl. Phys. **118**, 164901 (2015).
[10]S.-Y. Chiam, R. Singh, C. Rockstuhl, F. Lederer, W. Zhang, and A. A. Bettiol, Phys. Rev. B **80**, 153103 (2009).
[11]F. López-Tejeira, R. Paniagua-Domínguez, and J. A. Sánchez-Gil, ACS Nano **6**, 8989 (2012).
[12]C. Wu, A. B. Khanikaev, R. Adato, N. Arju, A. A. Yanik, H. Altug, and G. Shvets, Nat. Mater. **11**, 69 (2012).
[13]W.-S. Chang, J. B. Lassiter, P. Swanglap, H. Sobhani, S. Khatua, P. Nordlander, N. J. Halas, and S. Link, Nano Lett. **12**, 4977 (2012).
[14]M. Amin, M. Farhat, and H. Bağcı, Sci. Rep. **3**, 2105 (2013).
[15]N. Papasimakis and N. I. Zheludev, Opt. Photonics News **20**, 22 (2009).
[16]M. Kauranen and A. V. Zayats, Nat. Photonics **6**, 737 (2012).
[17]C. Argyropoulos, P.-Y. Chen, F. Monticone, G. D'Aguanno, and A. Alù, Phys. Rev. Lett. **108**, 263905 (2012).
[18]A. Attaran, S. D. Emami, M. R. K. Soltanian, R. Penny, F. behbahani, S. W. Harun, H. Ahmad, H. A. Abdul-Rashid, and M. Moghavvemi, Plasmonics **9**, 1303 (2014).
[19]J. Li, R. Yu, C. Ding, and Y. Wu, Phys. Rev. A **93**, 023814 (2016).
[20]Y.-F. Xiao, V. Gaddam, and L. Yang, Opt. Express **16**, 12538 (2008).
[21]Y.-F. Xiao, M. Li, Y.-C. Liu, Y. Li, X. Sun, and Q. Gong, Phys. Rev. A **82**, 065804 (2010).
[22]C. M. Bender and S. Boettcher, Phys. Rev. Lett. **80**, 5243 (1998).
[23]K. G. Makris, R. El-Ganainy, D. N. Christodoulides, and Z. H. Musslimani, Phys. Rev. Lett. **100**, 103904 (2008).
[24]C. E. Rüter, K. G. Makris, R. El-Ganainy, D. N. Christodoulides, M. Segev, and D. Kip, Nat. Phys. **6**, 192 (2010).
[25]R. El-Ganainy, K. G. Makris, D. N. Christodoulides, and Z. H. Musslimani, Opt. Lett. **32**, 2632 (2007).
[26]R. El-Ganainy, K. G. Makris, M. Khajavikhan, Z. H. Musslimani, S. Rotter, and D. N. Christodoulides, Nat. Phys. **14**, 11 (2018).
[27]L. Chang, X. Jiang, S. Hua, C. Yang, J. Wen, L. Jiang, G. Li, G. Wang, and M. Xiao, Nat. Photonics **8**, 524 (2014).
[28]B. Peng, Ş. K. Özdemir, F. Lei, F. Monifi, M. Gianfreda, G. L. Long, S. Fan, F. Nori, C. M. Bender, and L. Yang, Nat. Phys. **10**, 394 (2014).
[29]R. Fleury, D. Sounas, and A. Alu, Nat. Commun. **6**(1), 5905 (2015).
[30]X. Zhu, H. Ramezani, C. Shi, J. Zhu, and X. Zhang, Phys. Rev. X **4**, 031042 (2014).
[31]A. Ruschhaupt, F. Delgado, and J. G. Muga, J. Phys. A **38**, L171 (2005).
[32]P.-Y. Chen and J. Jung, Phys. Rev. Appl. **5**, 064018 (2016).
[33]G. Castaldi, S. Savoia, V. Galdi, A. Alù, and N. Engheta, Phys. Rev. Lett. **110**, 173901 (2013).
[34]S. Savoia, G. Castaldi, V. Galdi, A. Alú, and N. Engheta, Phys. Rev. B **89**, 085105 (2014).


Published under license by AIP Publishing

[35]Z. Lin, J. Schindler, F. M. Ellis, and T. Kottos, Phys. Rev. A **85**, 050101 (2012).
[36]J. Schindler, A. Li, M. C. Zheng, F. M. Ellis, and T. Kottos, Phys. Rev. A **84**, 040101 (2011).
[37]J. Schindler, Z. Lin, J. M. Lee, H. Ramezani, F. M. Ellis, and T. Kottos, J. Phys. A **45**, 444029 (2012).
[38]H. Li, A. Mekawy, A. Krasnok, and A. Alù, Phys. Rev. Lett. **124**, 193901 (2020).
[39]Z. Xiao, Y. Rádi, S. Tretyakov, and A. Alù, Research 2019, 7108494.
[40]M. Sakhdari, M. Hajizadegan, and P.-Y. Chen, Phys. Rev. Res. **2**, 013152 (2020).
[41]P.-Y. Chen and R. El-Ganainy, Nat. Electron. **2**, 323 (2019).
[42]M. Sakhdari, M. Hajizadegan, Q. Zhong, D. N. Christodoulides, R. El-Ganainy, and P.-Y. Chen, Phys. Rev. Lett. **123**, 193901 (2019).
[43]P.-Y. Chen, M. Sakhdari, M. Hajizadegan, Q. Cui, M. M.-C. Cheng, R. El-Ganainy, and A. Alù, Nat. Electron. **1**, 297 (2018).
[44]L. Feng, Y.-L. Xu, W. S. Fegadolli, M.-H. Lu, J. E. B. Oliveira, V. R. Almeida, Y.-F. Chen, and A. Scherer, Nat. Mater. **12**, 108 (2013).
[45]Z. Lin, H. Ramezani, T. Eichelkraut, T. Kottos, H. Cao, and D. N. Christodoulides, Phys. Rev. Lett. **106**, 213901 (2011).
[46]X. Zhu, L. Feng, P. Zhang, X. Yin, and X. Zhang, Opt. Lett. **38**, 2821 (2013).
[47]D. L. Sounas, R. Fleury, and A. Alù, Phys. Rev. Appl. **4**, 014005 (2015).
[48]R. Fleury, D. L. Sounas, and A. Alù, Phys. Rev. Lett. **113**, 023903 (2014).
[49]M. Sakhdari, M. Farhat, and P.-Y. Chen, New J. Phys. **19**, 065002 (2017).
[50]J. Wiersig, Phys. Rev. A **93**, 033809 (2016).
[51]H. Hodaei, A. U. Hassan, S. Wittek, H. Garcia-Gracia, R. El-Ganainy, D. N. Christodoulides, and M. Khajavikhan, Nature **548**, 187 (2017).
[52]W. Chen, Ş. K. Özdemir, G. Zhao, J. Wiersig, and L. Yang, Nature **548**, 192 (2017).
[53]S. Longhi, Phys. Rev. A **82**, 031801 (2010).
[54]M. Sakhdari, N. M. Estakhri, H. Bagci, and P.-Y. Chen, Phys. Rev. Appl. **10**, 024030 (2018).


Published under license by AIP Publishing